ACS APPLIED POLYMER MATERIALS

pubs.acs.org/acsapm Article

Development of a Rubber Recycling Process Based on a Single-Component Interfacial Adhesive

Michelle A. Calabrese, Wui Yarn Chan, Sarah H. M. Av-Ron, and Bradley D. Olsen*

Cite This: *ACS Appl. Polym. Mater.* 2021, 3, 4849−4860 Read Online

ACCESS | Metrics & More | Article Recommendations | Supporting Information

ABSTRACT: A simple and cost-effective adhesive-based rubber recycling process was designed as an alternative to devulcanization. Interfacial bonding between vulcanized and virgin rubbers is improved by incorporating adhesives and coating processes during rubber reblending and reducing interfacial defects that cause premature failure. In flat laminates, the bond strength between vulcanized and virgin materials doubles when a vulcanizing fluid and thin adhesive layer are introduced. These components are combined into single-component adhesives (SCAs), which improve bond strength sixfold over no treatment, using half the raw material as the multilayer adhesive. When SCAs are coated onto vulcanized rubber particles prior to reblending, the best rubbers exhibit nearly 50% increases in mechanical strength and toughness vs the untreated control and statistically identical extensibility; all treatments improved mechanical strength. This simple, inexpensive, and scalable process can be implemented with one step beyond standard reblending and curing, providing a promising alternative to devulcanization for polymer recycling.

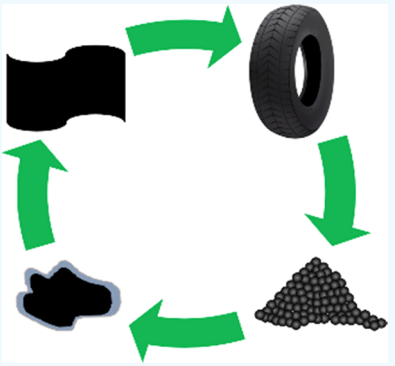

KEYWORDS: *recycling, rubber, devulcanization, isoprene rubber, composite, ground rubber*

1. INTRODUCTION

By 2040, the number of cars in service is expected to reach 2 billion globally,[1] highlighting the need for sustainable reclaiming methods for the millions of tons of waste tires generated each year.[2] Currently, no adequate reuse technology exists,[3−5] and in 2017, less than 25% of natural rubber (NR) from scrap tires was reused in ground rubber applications.[6]

The rubber industry uses a grind-and-blend process for recycling, where ground rubber particles (GRPs) produced from end-of-life tires are downcycled into fillers for various products.[7,8] Unlike thermoplastics that can be thermally reprocessed, sulfur-vulcanized NR is a thermoset that cannot melt without extensive chemical degradation. Accordingly, when GRPs are fused by compression molding without additives, only 35−40% of the original mechanical properties are recovered.[9,10] In spite of these inherent performance losses, using GRP as a partial substitute for virgin rubber in tire compounds has been attractive due to potential cost savings.

When vulcanized GRP is reblended with virgin rubber to form recycled composites,[11] the new material is chemically cross-linked, or cured, often using sulfur.[12] As the GRPs are already highly cross-linked, the mismatch in modulus and cross-linking density between the particles and the surrounding rubber matrix leads to poor bonding between the two materials. Upon subsequent deformation, the GRPs act as defects. Delamination of the virgin rubber matrix at the GRP interface due to poor bonding and adhesion then leads to poor mechanical properties.[13,14] These performance losses limit the allowable recycled content to roughly 5% in new tires and tire products,[8] though two reviews note industrial testing in which up to 10% of recycled rubber was incorporated with minimal performance losses.[15,16]

The most common strategy to reduce the cross-linking density mismatch between the GRP and the surrounding matrix is to add a GRP devulcanization step prior to reblending.[13] The goal of devulcanization is to cleave the sulfur−sulfur or carbon−sulfur bonds formed during the original vulcanization process. In theory, cleaving only the sulfur bonds decomposes the network into shorter, more processable chains without cleaving the backbone bonds and sacrificing mechanical integrity. Accordingly, devulcanization is considered the gold-standard technology for rubber recycling, despite its high costs.[17] However, in addition to high costs, devulcanization-based recycling processes have yet to achieve mechanical performance near that of virgin rubber.[18−20]

In practice, vulcanized rubbers are difficult and costly to process, and common devulcanization processes result in carbon−carbon bond cleavage in addition to the desired sulfur−sulfur or sulfur−carbon bond cleavage. Physical,[21] chemical, and microbial[22,23] devulcanization methods have been widely studied to improve the properties of recycled

Received: May 7, 2021
Accepted: August 21, 2021
Published: September 21, 2021

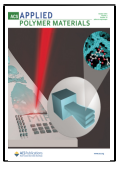

https://doi.org/10.1021/acsapm.0c01343
ACS Appl. Polym. Mater. 2021, 3, 4849−4860

material and increase the recycled content of new products. Physical methods of breaking rubber cross-links include microwave[24,25] and ultrasonic[26] devulcanization. Although S−S and S−C bonds are weaker than C−C bonds,[27,28] mechanical devulcanization leads to nonspecific bond cleavage, randomly breaking both cross-links and backbone bonds.[29] The devulcanized material often consists of shorter carbon backbone chains[9] than the virgin rubber, leading to weaker mechanical properties. In chemical devulcanization, a variety of reclaiming agents, including sulfides,[30,31] thiols,[32,33] and amino compounds,[34,35] are mixed in with GRPs with processing oil.[19,36] These processes only lead to surface devulcanization of the GRP.[37] In addition to its limited scalability, this method also releases toxic byproducts during the devulcanization process.[38] More recently, supercritical CO_2 has been studied[39,40] as an alternative to organic solvents for swelling GRPs, with promising results. Regardless, chemical devulcanization is often more expensive than physical methods due to high reagent[17] and energy[41] costs. Finally, microbial devulcanization methods have been explored but have limited utility due to the long time required to obtain significant devulcanization[42] and, like chemical processes, limit devulcanization to the surface of GRPs only.[43]

One alternative to devulcanization is to improve incorporation of the GRPs into the polymer matrix by GRP surface modification, thereby minimizing defects that spur delamination. This compatibilization strategy has been widely explored when incorporating GRPs in thermoplastic polymer blends to form composites known as thermoplastic vulcanizates (TPVs), and similar strategies are common in industrial particle-filled polymeric composites.[44] Polyethylene and polypropylene-based TPVs are most commonly investigated,[45,46] where compatibilization is required to obtain satisfactory mechanical properties, resulting from improved mixing uniformity and reduced GRP agglomeration.

To compatibilize GRPs with the thermoplastic polymer matrix, GRP surface modification has been extensively studied using both reactive and nonreactive compatibilizers. To modify the chemistry or polarity of GRP surface, reagents such as acrylamide,[47] allylamine,[48] maleic anhydride,[49] and others[50,51] are often used alongside radiation to promote reaction with the GRP surface; in many cases, dicumyl peroxide is used as a photoinitiator.[49,52] Chemically modifying the GRP surface can enhance interfacial adhesion with the polymer matrix, improve particle dispersion, and provide a reactive group for subsequent covalent bonding.[52,53] To further increase adhesion between GRPs and the surrounding thermoplastic matrix, a third polymer is often added to the blend as a compatibilizer. Adding copolymers such as methacrylic anhydride-grafted polypropylene or ethylene[47,53] and ethylene-1-octene[54,55] to TPVs significantly enhances mechanical properties. Scanning electron microscopy (SEM) shows that the copolymer compatibilizer often encapsulates the GRP, and the interfacial layer improves bonding between GRP and the surrounding polymer matrix.[54,56] Blending in ethylene propylene diene monomer rubber (EPDM) also tends to encapsulate the GRPs, improving GRP dispersion and adhesion between phases.[57,58] The diene comonomer also enables subsequent sulfur vulcanization and cross-linking with the surrounding matrix.

Though many report using these compatibilizing strategies for formulating GRP-filled TPVs, few studies have successfully applied these methods to incorporate GRP into virgin rubber. Previous attempts at GRP surface modification, including chlorination and surface polymer chain grafting, have been used with little success in rubber compounds.[59] Chlorination successfully improves GRP incorporation in nitrile-butadiene rubbers but causes embrittlement in NR.[60] When ethyl acrylate was grafted to the GRP surface in butadiene rubbers, poorer mechanical performance also resulted.[61] In each of these works, at least one critical mechanical performance metric was sacrificed when surface modification was used to improve another property, making these strategies largely infeasible.

Alternative surface modification strategies focused on adhesion and interfacial bonding have been successfully demonstrated by the tire repair industry. In current practice, two vulcanized rubbers are patched or rebonded for tire retreading[62] using an interfacial layer[28] and a vulcanizing fluid. An initially uncured, interfacial cushion gum (CG) layer is required to obtain strong bonding and cohesively dissipate tear energy between the two rubbers.[63] Cushion gum is a commonly used rubber filler already containing all of the chemical components necessary for proper vulcanization (see composition in Supporting Information XIX). While this method has only been applied to bond two vulcanized rubbers, the same concept could have value in blending ground rubber particles into virgin rubber.

Here, a new single-component rubber adhesive is developed and applied to improve the bond strength between cured and uncured rubbers in the recycling process, leading to improved performance for GRP recycling. Initially, the efficacy of various developed adhesive formulations is evaluated using flat rubber laminate strips as a model system, where one strip is composed of vulcanized rubber and one is composed of uncured, virgin rubber.[64] The laminate geometry is used to develop a single-component adhesive (SCA) to replace the current multilayer methodology, leading to an adhesive that is easily applied in an industrial particle coating process. The newly developed SCAs are then coated onto vulcanized GRPs prior to reblending with the virgin compound, and the mechanical properties of the composite materials are evaluated after blending and vulcanization. Significant performance gains are still achieved for a wide variety of process variables explored, suggesting that this rubber coating process shows significant promise as a new method of rubber recycling.

2. EXPERIMENTAL SECTION

2.1. Materials. All materials were used as received. Fast dry vulcanizing fluid 760 (cement) and cushion gum (CG) were obtained from Tech Tire Repairs. Two types of CG with nominal thicknesses of 1/16″ (actual 2 mm) and 1/32″ (actual 1 mm) were obtained. The CG thickness, d_{CG}, referred to throughout this work is the actual thickness measured by calipers. Tetrahydrofuran (THF, OmniSolv, >99.9%) was obtained from Millipore Sigma, and toluene (TOL) was obtained from Macron Fine Chemicals. *N-tert*-Butyl-2-benzothiazyl sulfenamide (TBBS, 97%) and zinc oxide (ZnO, 99.9%) were purchased from Alfa Aesar, stearic acid was purchased from TCI (>98%), and sulfur was obtained from Strem Chemicals Inc. Sundex 750T rubber processing oil (composed of heavy paraffinic distillate solvent from petroleum extract) was obtained from Holly Frontier, aliquoted upon receipt, and stored at −20 °C.

2.2. Cement and Cushion Gum (CG) Composition Analysis. Samples of ∼10 g cement were massed and subsequently frozen with liquid nitrogen and lyophilized for 72 h to remove nonsolids. Samples were then remassed to determine the solid fraction (7.0%). The polymer remaining after freeze-drying was analyzed via gel permeation chromatography (GPC) using THF as the mobile phase. The number-average molar mass, M_n, was 1.19×10^5 g/mol based on polystyrene standards with a polydispersity index of $Đ = 7.63$

https://doi.org/10.1021/acsapm.0c01343
ACS Appl. Polym. Mater. 2021, 3, 4849−4860

(Supporting Information I). Using supplier documentation and CHNS elemental analysis (Supporting Information II), the cement composition by mass was estimated as 93% of solvent (C_5–C_{10} saturated hydrocarbons), 5% of rubber polymer, and 2% of accelerator zinc bis(dibutyldithiocarbamate). To estimate the composition of CG, thermogravimetric analysis (TGA) was performed. Degradation profiles suggest that the CG contains roughly 9% of oil/small molecules and 28% of carbon black (Supporting Information XIX).

2.3. Preparation of Model Rubber Compounds. The model rubber vulcanizate used to simulate tire rubber, referred to as F3, contains carbon black and other additives listed in Table 1. The

Table 1. F3 Additive and Cure Package Formulation Denoted in phr (Parts per Hundred Grams of Rubber on a Mass Basis, the Rubber Industry Standard Unit)

additive	formula/type	phr
carbon black	N330	40
sulfur	S_8	1.25
stearic acid	$C_{18}H_{36}O_2$	2.00
zinc oxide	ZnO	2.00
Naugard butylated hydroxytoluene (BHT)	$C_{15}H_{24}O$	1.00
N-tert-butyl-2-benzo thiazolosulfenamide (TBBS)	$C_{11}H_{14}N_2S_2$	0.83

polymer is a high-cis (>95%) polybutadiene rubber (Lanxess, neodymium-catalyzed solution polymerization) with a number-average molar mass, M_n, of 1.28×10^5 g/mol based on THF GPC referenced to polystyrene standards with $Đ = 4.37$ (Supporting Information I). All model F3 rubber compounds as detailed below were prepared at the Akron Rubber Development Lab (ARDL) and stored at −20 °C when not in use.

Masterbatch F3. High-cis polybutadiene rubber was compounded with carbon black N330, stearic acid, zinc oxide, and antioxidant in proportions detailed in Table 1 in a Banbury rubber compounding mixer at 65.5 °C and 55 rpm for 4.5 min. Mixed compounds were placed on a roll mill at 50 °C, with three cuts on each side and three end passes for the sheet to cool. The F3 additive formula is similar to other curing packages used in the literature.[31,35,37,38]

Uncured F3. Masterbatch F3 was loaded into the Banbury mixer operating at 40 °C and 50 rpm. Sulfur and TBBS were loaded after 1 min, proportions of which are detailed in Table 1. The rotor speed was adjusted to 40 rpm to keep the temperature at around 75 °C, and mixing was complete in 5 min. Mixed compounds were placed on a roll mill at 21 °C, with three cuts on each side and three end passes for the sheet to cool.

Cured F3. The uncured F3 was vulcanized in a hydraulic press at a temperature of 160 °C for 40 min, in accordance with the ASTM D3182. Optimum cure time (t_{90}, time required to reach 90% of the maximum achievable torque) was determined to be 39 min, using a moving die rheometer in accordance with the ASTM D2084.

Ground Rubber Particle (GRP) F3. For ground rubber particle (GRP) reblending studies, cured F3 was cryoground to two mesh sizes and sorted with standard mesh filters: 250–500 μm (medium, No. 35 mesh) used for the screening trials and <250 μm diameter (small, No. 60 mesh) used for the final trials.

F3 Rubber Strips. Rectangular rubber strips measuring 76.2 mm × 12.7 mm (small) or 152.4 mm × 25.4 mm (large) were used to prepare laminates for T-peel adhesion tests. Each strip was composed of an approximately 2 mm thick F3 layer and a 1.5 mm thick backing layer. Compositions of the F3 layer for cured F3 strips and uncured F3 strips were identical to cured F3 and uncured F3, respectively. Backing layers were composed of nylon cord-reinforced rubber. Backing layers were added to prevent the strip from deforming and stretching during T-peel testing, such that only the interfacial bond strength was measured.

2.4. Preparation of the Single-Component Adhesive (SCA). All adhesives are composed of vulcanizing fluid (cement) and cushion gum (CG). Single-component adhesives (SCAs) were prepared by combining these two components either with or without solvent addition, using one of three methods depicted in Figure 1.

Wet Preparation. A wet blending approach was designed to combine the CG and cement by codissolving both components in THF or toluene (Figure 1a). The CG was dissolved over 5 days using 4.5 mL of solvent per gram CG. Complete dissolution was confirmed by visual inspection with no observation of large chunks in the solution. Aging studies comparing concurrent dissolution of both components and the addition of cement only after CG had fully dissolved showed that the latter process potentially improved adhesive effectiveness (Supporting Information X); this preparation method was subsequently adopted. Two wet SCA formulations were prepared with either 0.23 or 0.45 mL cement per gram CG (see Supporting Information IV). The SCA in solvent was used in laminate adhesion studies only; SCA was evaporated to dryness in all other studies.

Evaporated Method. SCA in solvent was prepared using the aforementioned wet preparation method. The mixture was subsequently poured into a flat, square mold and evaporated to dryness overnight under ambient conditions in a fume hood with high air circulation (Figure 1b). The SCA was removed from the mold as a single sheet and massed to confirm full solvent evaporation. The volume of wet SCA used in the casting process was adjusted to obtain sheets of different thicknesses and density of total solids.

Dry Blending Preparation. The dry blending of CG and vulcanizing cement were performed without solvent addition in a Brabender 3-piece mixer (60 mL capacity, Banbury mixing blades) with the ATR Plasti-corder rheometer drive system (Figure 1c). The mixer starting temperature and mixing speed were set to 40 °C and 40 rpm, respectively. First, 40 g of CG was loaded into the mixer and masticated for 1 min, followed by the addition of either 20 or 10 mL of vulcanizing cement (0.50 mL/g of CG and 0.25 mL/g of CG, respectively). Mixing was performed for a further 4 min. As the cement is composed mostly of solvent, the two-component mixture appeared wet when it was removed from the mixer. The SCA mixture was then flattened and passed through a Brabender two-roll mill at least five times at ambient temperatures to allow further mixing and solvent evaporation, until the dry blend SCA texture resembled that of CG. The dry blend SCA showed promise in initial particle reblending

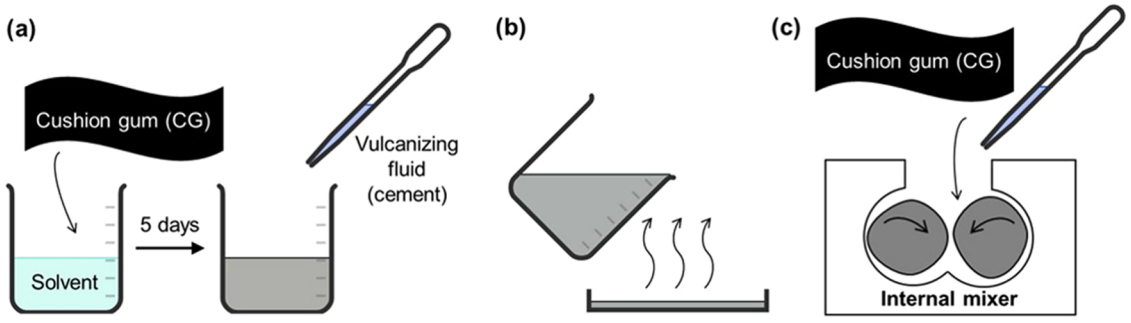

Figure 1. Preparation of the SCA using the (a) wet preparation, (b) evaporated, and (c) dry blending preparation methods.

https://doi.org/10.1021/acsapm.0c01343
ACS Appl. Polym. Mater. 2021, 3, 4849–4860

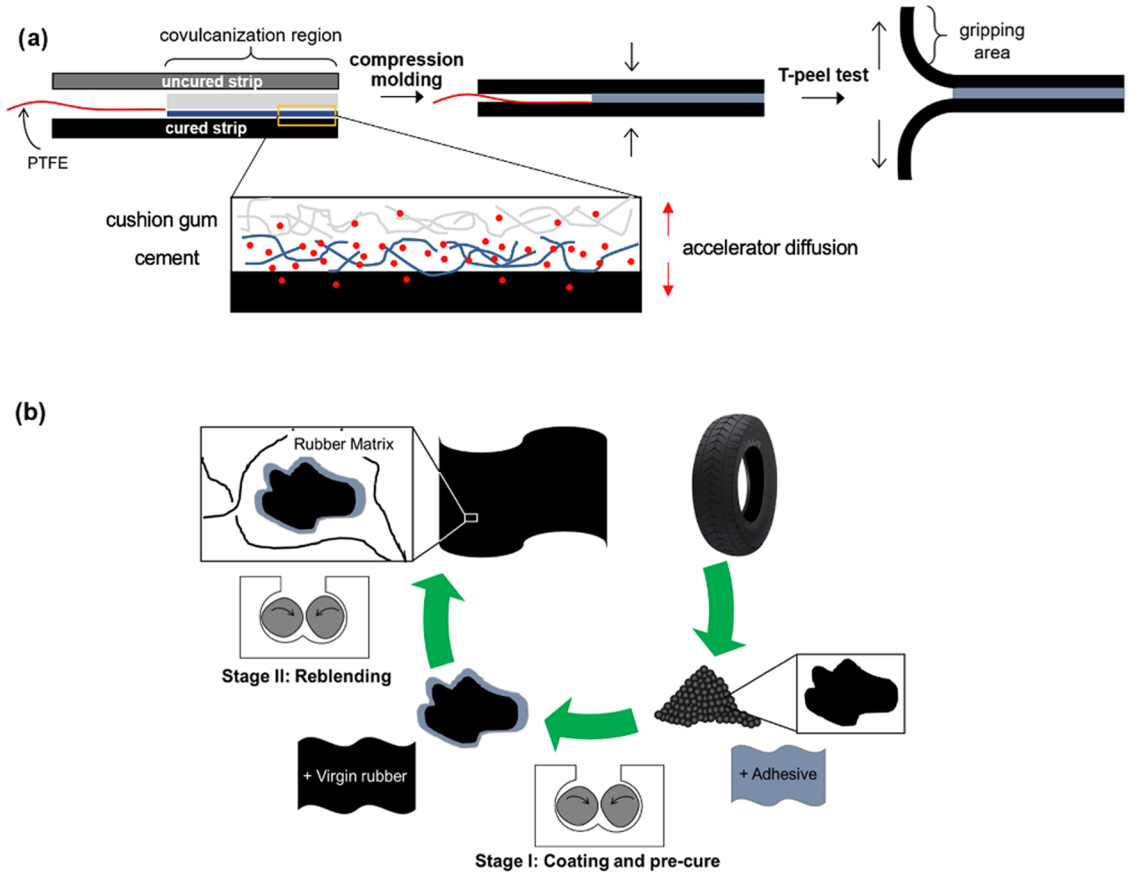

Figure 2. Schematic of the two-component adhesive laminate assembly (a) and ground rubber particle coating and reblending (b).

Table 2. Formulation Ranges Tested in TCA Laminates

d_{CG} (mm)	mL cement/g CG	g cement solids/g CG	$\rho_{A,CG}$ (g CG/m^2)	$\rho_{A,solids}$ (g solids/m^2)
1	0.45−3.6	0.02−0.2	970	1000−1160
2	0.23−1.8	0.01−0.1	1950	1970−2140

studies (Supporting Information XV) and thus was used in further reblending trials (Section 3.3).

2.5. Preparation of Laminate Assemblies for T-Peel Adhesion Tests. T-peel adhesion tests were used to explore the degree of bonding achieved between vulcanized and uncured rubbers. Cured F3 strips were bonded to uncured F3 strips with adhesives applied over the bonding area (Figure 2a). To have sufficient gripping area on the laminates for T-peel tests, adhesives were only applied over approximately 60% of the strip length, the covulcanization region. The covulcanization region was 44.5 (L) mm × 12.7 (W) mm and 88.9 (L) mm × 25.4 (W) mm for the small and large laminates, respectively. A thin poly(tetrafluoroethylene) (PTFE) film was placed between the two sheets in the untreated region (∼40%) to prevent bonding in the gripping area. Prior to laminate assembly, the surface of the cured laminates was hand-buffed with a coarse silicon carbide buffing stone until the surface appeared uniformly matte. Methods of adhesive application for each type of adhesive are shown in Figure 2.

Two-Component Adhesive (TCA). Cement and CG were applied sequentially as separate layers. Primary experiments were conducted at a cement loading of 0.45 mL/g CG (0.02 g of cement solids/g CG) using 2 mm thick CG. Here, the CG areal density was $\rho_{A,CG}$ = 1950 g CG/m^2, and the areal density of total solids (CG and cement solids) was $\rho_{A,solids}$ = 2000 g solids/m^2. The ranges of all conditions tested, including experiments using 1 mm CG, are listed in Table 2. Supplemental experiments (Supporting Information VI) showed that operating outside of the parameter ranges listed in Table 2 was not beneficial to bonding.

Wet Preparation SCA. A syringe was used to dispense the dissolved SCA onto the cured laminate surface in 1 mL increments. The strip surface was allowed to dry for ∼5 min before spreading the next increment. To achieve an adhesive layer with the same areal CG and solids' density as the primary TCA experiments ($\rho_{A,CG}$ = 1950 g CG/m^2 and $\rho_{A,solids}$ = 2000 g/m^2, respectively), a wet SCA volume of ∼6 mL was required. The solids' areal density in the wet preparation laminates ranged from $\rho_{A,solids}$ = 330 to 2000 g solids/m^2. After applying the final SCA increment, the strip surface was allowed to dry for at least 18 h. Before curing, the uncured strip was placed on top of the dried, SCA-coated strip.

Evaporated Method SCA. The evaporated method SCA sheet was cut into strips with the same dimensions as the covulcanization region and sandwiched between the cured and uncured F3 strips. The mass of the evaporated SCA strip was used to determine the solids' areal density, which ranged from $\rho_{A,solids}$ = 890 to 1980 g solids/m^2. To confirm uniform thickness, d_{SCA}, across the SCA strip, each end was measured with a caliper. While d_{SCA} values were similar, accurate measurements were difficult due to the flexible nature of the dried SCA.

2.6. Laminate Assembly Curing. Laminates were placed in a 12-slot (small) or 4-slot (large) stainless steel mold (see Supporting Information III) with the cured side up and covulcanized at 160 °C for 20 min at a high pressure (6.5−10.3 MPa). The laminate assembly height was at least 0.75 mm thicker than the mold to ensure sufficient applied pressure. Following cocuring, the area protected by the PTFE film easily separates.

https://doi.org/10.1021/acsapm.0c01343
ACS Appl. Polym. Mater. 2021, 3, 4849−4860

Table 3. 2^5 Factorial Design of the Particle Recycling and Reblending Experiment

factor tested	base care	trial level
(1) cement concentration in mL cement per g CG in SCA composition	0.5 mL/g of CG	0.25 mL/g of CG
	procedure:	at t = 0 min: add cushion gum to mixer
	temperature: 40 °C	at t = 1 min: add rubber cement to the mixer
	mixing speed: 40 rpm	total mixing time: 5 min
(2) coating process in the mixer	temperature: 60 °C	temperature: 80 °C
	mixing speed: 40 rpm	mixing speed: 40 rpm
	after 4.5 min, set to 60 rpm	
	mixing terminated 5 min after torque spike	mixing terminated 15 min after torque spike
	total mixing time: 10−15 min	total mixing time: 20−25 min
(3) pretreatment of the coated GRP	10 min procure at 80 °C	no treatment
(4) reblending process in the mixer	temperature: 65 °C	temperature: 60 °C
	mixing speed: 60 rpm	mixing speed: 30 rpm
	after 2.5 min, set to 40 rpm	
	total Mixing time: 9 min	total Mixing time: 10 min
	procedure	at t = 0 min: add virgin rubber to the mixer
		at t =1 min: add the coated GRP in the mixer
		at t =5 min: add the curing package to the mixer
		at t = 7 min: blow compressed air into the system
(5) curing time	20 min at 160 °C	15 min at 160 °C

2.7. Particle Recycling Process. The particle recycling process occurred in two mixing stages (Figure 2b). GRPs were coated with SCA in the first stage; the coated GRPs were then reblended with the uncured masterbatch F3 with curing agents. The full particle recycling reblending process can be split into five steps: (1) formulation of SCA, (2) coating of GRP, (3) pretreatment of the coated GRP, (4) reblending with the uncured rubber, and (5) curing. A 2^5 factorial design was used to investigate these five parameters, where each factor followed either the "base case" or "trial level" described in Table 3.

Coating Process. GRP and SCA prepared via dry blending were combined in the Brabender mixer, with the temperature, mixing time, and mixing speed dictated by the base-case or trial-level coating process in Table 3. SCA formulations with two cement concentrations were used: 0.5 mL of cement/g CG (base case) and 0.25 mL/g of CG (trial level). To keep the cushion gum per mass of GRP constant, SCA was added at a weight ratio of GRP to SCA of 10:1 or 10:0.86 for the base case and trial level, respectively.

Pretreatment of Coated GRP. The day after particle coating, GRPs were either pretreated with heat or were left untreated. In the base case, all coated GRPs are precured for 10 min at 80 °C in an oven.

Reblending Process. Reblended samples were made with 15 phr of recycled GRP relative to the virgin rubber based on the bare (uncoated) particle mass. The curing package consisted of 1.25 phr of sulfur and 0.83 phr of accelerator TBBS. Two conditions each were investigated for temperature, mixing speed, and mixing time, as detailed in Table 3. Sample torque curves from the Brabender mixer during both coating and reblending are given in Supporting Information XVII. A two-roll mill at the same temperature as the mixer was used to complete the compounding process. Reblended rubber was passed through the mill six times, with alternating folds length- and width-wise.

Curing. The material was pressed into 1.55 mm thick plaques in a Carver hydraulic press at 160 °C for up to 20 min at a pressure between 24 and 31 MPa.

2.8. Fabrication of Positive and Negative Controls. Three control rubber plaques were made for comparison with the reblended rubber containing GRP. The positive controls are vulcanized rubber plaques containing no GRP. Two no-particle controls were prepared using the base-case and trial-level reblending processes. A negative control was prepared using the uncoated GRP with the base-case reblending process. All controls were cured for 20 min.

2.9. Mechanical T-Peel Adhesion Tests and Tensile Testing. Mechanical testing was performed on a Zwick Z2.5 mechanical tester equipped with a 500 N load cell; coarse sandpaper was applied to the grip surface when appropriate to mitigate slip. T-peel tests were performed following the ASTM D1876 conditions (with the exception of sample dimensions). A separation speed of 50 mm/min was used for all tests. Control laminate assemblies were prepared periodically to confirm that all assembly, pressing, and mechanical testing methods were performed consistently over time. In strongly bonded laminates, slip occasionally occurred midway through a peel test. In this case, all data after the onset of slip was removed. A weighted average of the T-peel tests based on the travel distance between the first and last peaks was used to calculate average parameters. Laminate surfaces were photographed after peel tests (Figure 3a).

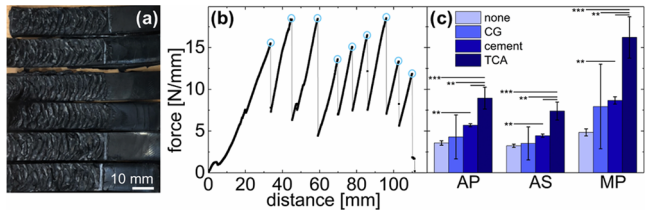

Figure 3. Laminate T-peel test results. (a) Strip surfaces after peeling with deep wrinkles and material transfer between sides indicate strong bonding. (b) Peel force vs travel distance. A MATLAB routine identifies peaks (circles). (c) Laminate MP, AS, and AP for various treatments: none, CG (no cement), cement (no CG), TCA (see Supporting Information VII).

A MATLAB routine was developed to analyze T-peel test data; an example of the analysis and a T-peel test force curve are shown in Figure 3b. The algorithm identifies the location and values of the peaks (blue circles in Figure 3b) and then identifies the maximum peak value (MP), the peak average value (PA, average of all blue circled peaks), and the average strength (AS, average force between the first and last peaks). As is standard, values are reported in units of force per strip width (N/mm).

After particle reblending, micro-dumbbells ($N \geq 7$) were cut from the cured plaques using an ASTM D1708 microtensile die from Pioneer Die-tecs. A separation speed of 100%/min was used for all tests. For all samples, force curves were reproducible between trials with no significant outliers (Supporting Information XXIV).

https://doi.org/10.1021/acsapm.0c01343
ACS Appl. Polym. Mater. 2021, 3, 4849−4860

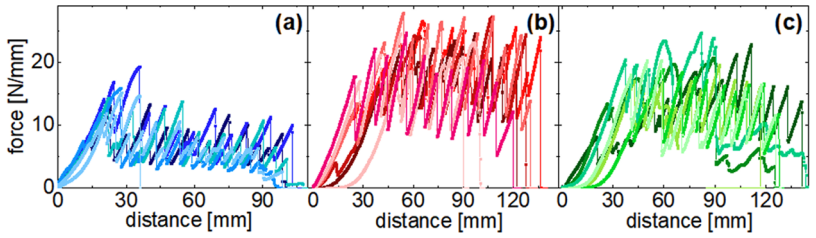

Figure 4. T-peel test raw data for laminates ($\rho_{A,solids} \approx 2000$ g CG/m^2) prepared with the two-component adhesive (a) or the single-component adhesive using the (b) wet method or (c) evaporated method. Here, 2000 g solids/m^2 corresponds to an interfacial layer thickness of ~2 mm.

MATLAB scripts for both analyses are given in Supporting Information XXV.

2.10. Statistical Analysis. Error bars on all figures correspond to ±1 standard deviation of the mean parameter, unless otherwise noted. Student's *t* tests were used to evaluate if the mean T-peel test parameters (average peak, average strength, maximum peak) were significantly different between any TCA or SCA formulations. Two-sided *t*-tests were performed in all cases, for clarity, when making comparisons across multiple laminate data sets. The null hypothesis was that the population means were equal, and the alternative hypothesis was that the means were not equal.

A similar analysis was conducted for the tensile testing results from the coated and reblended GRPs. One-sided *t*-tests were performed between the coated GRP-recycled material and the untreated GRP control for stress at break and toughness. As the treated samples had higher average values than the untreated control for these two metrics, the null hypothesis was that the population means were equal, and the alternative hypothesis was that the tensile parameter (maximum peak, peak average, average strength) was greater in the treated samples. To determine if performance gains were made without sacrificing elongation at break, a two-sided *t*-test was used between the coated samples and untreated control. Here, elongation values were similar between data sets.

One-sided *t*-tests were also used to compare tensile results between the base and trial controls, where the base case had higher average parameter values. As such, the alternative hypothesis was that each metric was greater for the base control. In all figures, statistical significance at the $p = 0.05$ level is indicated by the * symbol, at $p = 0.01$ by **, and at $p < 0.0001$ by ***.

3. RESULTS AND DISCUSSION

3.1. Proof-of-Concept Adhesive Bonding in Flat Rubber Laminates. The idea of an interfacial adhesive for GRP surface modification as an alternative to devulcanization is based on the current practice in the tire industry, where two vulcanized rubbers can be rebonded with a thin commercial adhesive and interfacial layer.[32] Initial experiments used a planar laminate geometry as a model system to enable development of an adhesive that is compatible with particle blending in a model system without the complexities of curvature, roughness, or shape irregularity that are present in particle-based systems (Figure 3).

Results from mechanical T-peel tests, shown in Figures 3 and 4a, demonstrate that in the two-component adhesive (TCA) system consisting of commercial cushion gum and vulcanizing cement, layers of both components are required to successfully bond the cured and uncured laminates with significant peel force (Figure 3c). A sample T-peel test force curve is shown in Figure 3b; large variations in force reflect stick-slip behavior during peeling. In addition to quantifying the maximum peak (MP), average peak (AP), and average strength (AS) values for each laminate, the strip surfaces were visually examined after peel testing. Surfaces of well-bonded laminates contained deep wrinkles and material transfer between the two sides of the strip (Figure 3a and Supporting Information XIV) indicative of primarily cohesive, as opposed to adhesive, failure. As a benchmark, multiple small uncured laminates ($N = 6$) were prepared and tested so that the virgin material bond strength could be quantified. For the virgin material, the average peak, maximum peak, and average strength (in N/mm) were 27.7 ± 3.9, 36.8 ± 4.2, and 25.9 ± 3.4, respectively (see Supporting Information XXI for T-peel test curves and values).

As shown in Figure 3c, bonding the two strips together using only CG (no cement) or only cement (no CG) results in low average peel strengths, maximum peaks, and average peak values. The CG-only formulation and no-treatment control were statistically identical for all metrics, and the cement-only formulation provided only marginal improvement over the no-treatment control. In the cement-only formulation, the cured laminate strip peeled easily away from the uncured surface. Little to no material transfer was observed, suggesting adhesive failure. However, when the TCA is used, the MP, AS, and AP values substantially improve, roughly doubling from the CG-only and cement-only controls and nearly tripling from the no-treatment controls. These results show clear improvements in bonding resulting from the TCA layer. While the TCA layer significantly improves interfacial bonding, it does not enable full recovery of mechanical properties observed in virgin rubber; the average strength of two bonded uncured laminates is roughly 4-fold larger than achieved with the TCA laminates. This gap in performance motivated further optimization of the TCA formulation, which required an understanding of the relevant formulation parameters and mechanism of bonding.

Laminate formulations ($N = 1$) were subsequently screened to determine the optimal formulation space, revealing that while each parameter significantly affected bonding, the average strength was always on the same order of magnitude when the CG areal density, cement concentration, oil addition, and surface roughness were varied. These screening studies are summarized in Supporting Information XX and IV. Studied parameters were the presence of oil, surface roughness, and ratios of CG and vulcanizing cement. Briefly, oil and rough surfaces were detrimental to bonding but the effects were minor (10−20% reduction in MP, AP, AS). Bond strength was independent of the CG areal density for the two conditions tested ($\rho_{A,CG} = 970$ and 1950 g CG/m^2), demonstrating that 50% less CG can be used to obtain equivalent bonding. Bond strength worsened at high cement concentrations (≥1.4 mL/g CG), and the cured surface peeled easily away from the CG and uncured sides, suggesting a transition from cohesive to adhesive failure. However, bond strength was independent of concentration over a large window (0.23−0.91 mL/g CG), saving cost and minimizing input raw materials. The relative insensitivity of the average strength to the cement concen-

https://doi.org/10.1021/acsapm.0c01343
ACS Appl. Polym. Mater. 2021, 3, 4849−4860

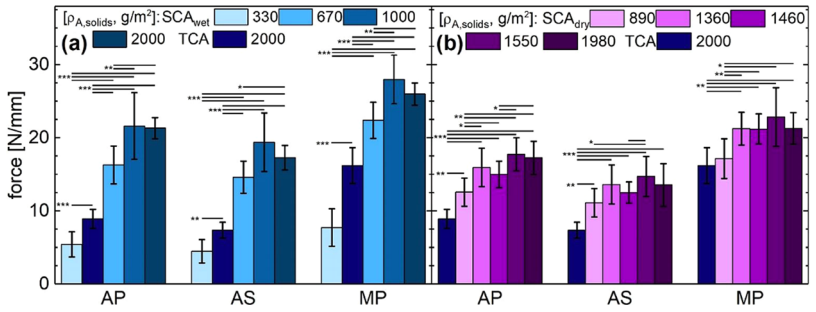

Figure 5. Average peak, average strength, and maximum peak for the two SCA preparation methods: (a) wet and (b) evaporated versus the TCA controls. SCA p-values vs no treatment were all $p < 0.0001$ and are thus not shown. Here, 1000 g solids/m^2 corresponds to an interfacial layer thickness of ∼1 mm (see Supporting Information IX, XI, and XXII).

tration suggests that accelerator diffusion is limited and that the majority of the accelerator remains in the TCA layer instead of interdiffusing into the cured laminate strip. However, interdiffusion does occur to a degree, as material transfer between laminate strips indicates cohesive failure, which results from interpenetration. At very high cement concentrations, adhesive failure appears to be promoted by overcuring of the already cured laminate strip. Further, a minimum areal density is likely required to achieve cohesive failure, as cement-only laminates with a near-zero layer thickness failed adhesively.

Though screening experiments identified optimal TCA formulations, no TCA formulation gave bond strengths approaching those of the uncured laminates (Supporting Information IV, VII, and XXI). One possible explanation for poorer bonding is that the accelerator distributes nonuniformly during the curing process. Results from screening trials suggesting that accelerator diffusion is limited are also supported by TCA trials showing that laminates with cement applied to both strips performed better than those with cement applied only to the cured surface (Supporting Information VII). As such, strategies to more evenly disperse the cement within the CG were subsequently pursued in hopes of improving bonding.

3.2. Development of Single-Component Adhesives (SCAs). Based on the gained understanding of the bonding mechanism, the adhesive formulations were adapted to improve laminate bond strength (Figure 4b,c). To simplify the adhesive application process to be compatible with particle coating and to more uniformly disperse the accelerator within the adhesive, a single-component adhesive (SCA) was developed. To form this adhesive, the cement and CG are blended together using various methods and then this single component is coated onto the rubber laminates. For the SCA trials summarized below, a cement loading of 0.45 mL/g CG was used; additional trials at 0.23 mL/g CG gave similar results (Supporting Information IX).

The developed SCA was applied to laminates ($N \geq 5$) using one of two methods, both of which resulted in improved peel parameters vs the TCA for a constant total adhesive loading of $\rho_{A,solids} \approx 2000$ g CG/m^2. The SCA was either applied while wet and allowed to dry before pressing (wet method) or evaporated to dryness before being added to the laminate as a flat strip (evaporated method). Figure 4 summarizes the T-peel test results from the TCA, wet SCA, and evaporated SCA at an equivalent areal density of total solids ($\rho_{A,solids} \approx 2000$ g solids/m^2). As seen in Figure 4, the wet SCA laminate preparation performs substantially better than the other two formulations and has average properties that are over twice as high as those of the TCA. The evaporated SCA also shows substantial improvements vs the TCA laminates but does not meet the performance of the wet SCA laminates. The bonding in the SCA laminates improved performance so substantially that the AP, MP, and AS values are at a level that is 75% of the uncured laminate values (see Figure 5). In comparison, TCA only achieved 30% of the uncured laminate value.

Many additional SCA formulations exceeded the TCA controls in the peel test performance, even when the quantity of adhesive, reported as the solids' areal density, was substantially lower. Unlike in the TCA studies where the areal density of CG and solids is set by the CG thickness, the solubilized or evaporated SCA can be applied to the laminate surfaces in finer increments. To explore the impact of areal density, i.e., layer thickness, different SCA volumes were applied to the laminate surfaces ($\rho_{A,solids}$ = 330−2000 g solids/m^2, equivalent thickness = 0.33−2 mm). Statistical analysis determined the minimum SCA solids' areal density required for improvements in performance vs the TCA and that required for equal performance to the baseline value of $\rho_{A,solids}$ = 2000 g solids/m^2 (Figure 5; see Supporting Information XXII and XXIII for T-peel test data).

As shown in Figure 5a for the wet SCA, using at least one-third the raw material mass ($\rho_{A,solids} \geq 670$ g solids/m^2) in the SCA leads to improved performance vs the TCA ($\rho_{A,solids}$ = 2000 g solids/m^2) in all three metrics ($p < 0.0001$). When one-sixth the raw material mass as the TCA is used in the wet SCA laminates ($\rho_{A,solids}$ = 330 g solids/m^2), improvements are gained vs the no-treatment controls (Supporting Information VIII); however, the TCA laminates give statistically better performance at this areal density of SCA (Figure 5). Follow-up wet SCA studies on large laminates examined even thinner layers ($\rho_{A,solids}$ = 80 g solids/m^2); these laminates showed performance improvements over no-treatment controls, even up to a 96% reduction in SCA solids' density relative to the quantity used for TCA (Supporting Information XII). This indicates that even remarkably thin SCA coatings can have an effect on adhesion.

Similar to the results seen in the screening studies for the TCA laminates, the performance in the wet SCA laminates plateaus with increasing the solids' areal density. At $\rho_{A,solids}$ = 1000 and 2000 g solids/m^2, the performance for all three peel test metrics is indistinguishable within experimental noise; both densities achieve performance at 75% of the uncured laminate values. Statistically significant differences in performance are observed between both of these conditions and the next-lowest areal density ($\rho_{A,solids}$ = 670 g solids/m^2),

https://doi.org/10.1021/acsapm.0c01343
ACS Appl. Polym. Mater. 2021, 3, 4849−4860

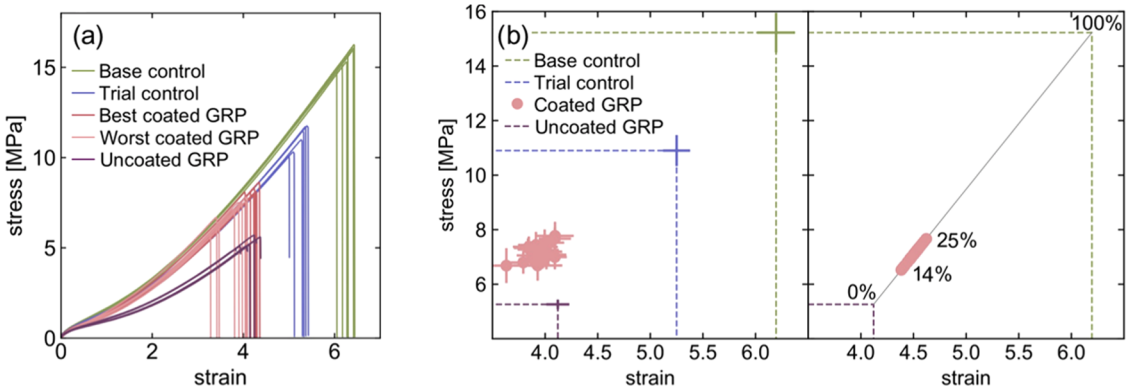

Figure 6. (a) Stress−strain curves for best- and worst-performing recycled rubbers with coated GRP and three controls: no particle (base, trial) and no treatment (base). (b) Left: stress and strain at break; error bars are the 95% confidence interval. Controls are plotted as dotted lines. Right: horizontal projection of stress at break on a progress percentage curve between the untreated particle and virgin material base controls.

indicating that the onset of the plateau occurs at solids' areal densities between 670 < $\rho_{A,solids} \leq$ 1000 g solids/m^2.

The evaporated SCA method, developed to mimic the industrial reblending process, which cannot easily handle large quantities of solvent, produced adhesion results that were qualitatively similar but quantitatively inferior to the wet SCA method. Similar to the wet laminates and the TCA screening studies, performance plateaued above a particular solid area density; an areal density of $\rho_{A,solids}$ = 1360 g solids/m^2 gave an equal performance to all evaporated method laminates with higher areal densities (Figure 5). Even the lowest areal density ($\rho_{A,solids}$ = 890 g solids/m^2) tested exceeded the performance of the TCA controls for the average peak and average strength metrics (Figure 5b; p < 0.01). However, the evaporated method laminates always underperformed the wet laminates, indicating that the presence of solvent is beneficial for bonding (see Supporting Information XXIII). Nevertheless, the evaporated method laminates perform exceedingly well vs all controls, providing confidence that a dry particle coating process could be implemented.

The shape of the laminate peel test curves (Supporting Information XXI−XXIII) indicates different mechanisms of bonding as a function of the solids' areal density (approximate layer thickness). While the shapes of the peel curves for cohesively and adhesively bonded laminates differ considerably from one another, they are quite similar to those seen for cohesively and adhesively failing epoxide adhesives, respectively.[65] In strongly bonded laminates, curve shapes indicate stick-slip behavior during peeling[66,67] (Figures 3b and 4) where the sample builds stress and then releases it during a sudden tearing/crack propagation event. The failure mechanism in the strongly bonded laminates is primarily cohesive,[67] as evidenced by the substantial material transfer between the sides of the laminate (Figure 3a and Supporting Information XIV). Deep wrinkling on the laminate surface also results during peeling. In the wet SCA laminates, this cohesive failure dominates when $\rho_{A,solids} \geq$ 1000 g solids/m^2, and in the evaporated method laminates, this behavior dominates when $\rho_{A,solids} \geq$ 1360 g solids/m^2. This minimum required solids' density to observe significant material transfer and cohesive failure suggests that substantial interpenetration and cross-linking between laminate strips contribute to the improved performance.

Conversely, laminates with lower bond strengths exhibit smoother curves with less dramatic peaks and valleys that suggest a different bonding mechanism[65] (Supporting Information XII, XIV, and XXII). These peel curves correspond to laminate surfaces that are substantially smoother and do not have a significant material transfer between sides or deep wrinkles (Supporting Information XII), supporting primarily adhesive failure. In the wet method laminates, adhesive failure dominates when $\rho_{A,solids} \leq$ 330 g solids/m^2, and a transition between the cohesive and adhesive failure is seen at $\rho_{A,solids}$ = 670 g solids/m^2. Similarly, features of both cohesive and adhesive failure are observed in the peel curves of the evaporated method laminates at $\rho_{A,solids}$ = 890 g solids/m^2. Interestingly, regions exhibiting material transfer are found in the wet laminates even when $\rho_{A,solids}$ = 330 g solids/m^2, suggesting that interpenetration and cross-linking between strips still occur to a degree at low solids' areal density. Indeed, a wet interface would enable the surrounding network to swell, thus increasing the diffusivity of polymer chains and leading to a stronger bond after dying and curing. While the transition between cohesive and adhesive failure is typically a strain rate-dependent phenomenon observed within a single material,[65−67] the totality of the peel test data indicates that this transition can also occur as a function of adhesive layer thickness. These results ultimately suggest that having a solids' areal density, i.e., layer thickness, above a minimum threshold is required for substantial interpenetration, cohesive failure, and ultimately good performance.

3.3. Improving Bonding in Reblended Ground Rubber Particles (GRPs). To improve interfacial bonding between ground rubber particles and virgin rubber, SCA was next applied to GRPs prior to the standard rubber reblending process. To incorporate SCA, the conventional process was modified to two stages, illustrated in Figure 2b: GRP coating with adhesive and coated particle reblending with the virgin compound. The current practice for particle recycling and reblending occurs without the first coating step;[68] however, the mechanical properties of the resulting material are substantially reduced. As the GRP content has been limited to between 5% and 10%[6] to maintain mechanical integrity in various applications, SCA material performance using a higher GRP fraction (15 wt %) was evaluated with respect to five factors illustrated in Figure 2b: (1) SCA formulation, (2) coating process, (3) particle pretreatment, (4) reblending process, and (5) cure time.

The specific process elements explored were selected based on their hypothesized role in interfacial bonding, and an

https://doi.org/10.1021/acsapm.0c01343
ACS Appl. Polym. Mater. 2021, 3, 4849−4860

extensive 25 factorial design was implemented to help understand the role of each of the five factors on the mechanical performance of the reblended material as quantified by the toughness, and elongation and strength at break (Table 3). Exploring the base-case and trial-level parameters led to 24, as opposed to 32, total conditions (see Supporting Information XVI), as particles coated with the base-case condition (factor 3) were always precured (factor 4). The base-case coating process employed lower temperatures than the trial level to prevent precuring during mixing. As the SCA layer and GRP are subjected to high shear forces during the reblending step (stage II), precuring treatment after GRP coating was designed to keep the SCA layer intact via light cross-linking to the GRP surface. The trial level aimed to decrease material use, simplify the procedure, and minimize the number of steps. An SCA formulation with less cement was used, mixing speeds were constant within each stage, and the precuring step was incorporated into the coating process by increasing the temperature. The trial level also attempted to keep the SCA layer intact by reducing the mixing speed for reblending to 30 rpm. To account for differences in the mixing processes, two no-particle controls were prepared using the parameters for the base case and trial level, as described in Section 2.8.

Results from all coating and reblending trials in the factorial design are summarized in Figure 6, where both the best- and worst-performing conditions lead to improvements in the stress at break vs the untreated controls (Figure 6b, $p < 0.001$). The top two performing conditions have average strength and toughness values that are over 45% larger than the no-treatment controls. Nine of the 24 conditions resulted in an average stress at break that was over 40% higher than the no-treatment controls. These performance improvements validate the effectiveness of applying the SCA coating to improve interfacial bonding. A table of values for stress, elongation, and toughness at break and p-values for each of the three parameters are given in Supporting Information XVI.

All coated samples had average stress-at-break (Figure 6b, left) values that were statistically larger than the untreated control, though elongation at break did not improve. Toughness also significantly improved for all but the worst-performing sample ($p = 0.09$; see Supporting Information XVI). Figure 6b (left) shows the average stress and elongation at break of each coated sample and the controls. The stress−strain curves for the highest performing condition clearly show improved toughness and stress at break without sacrificing extensibility vs the no-treatment control (Figure 6a), whereas the curves for the worst-performing condition show a slight decline in elongation at break. The highest performing sample corresponds to the base case for factors 1−3, while the worst sample corresponds to base-case conditions for all but factor 4. Overall, two-thirds of the coated samples (16 of 24) showed statistically significant improvements in the stress at break and toughness with no detrimental impact on the elongation at break.

A progression scale based on stress at break, shown in Figure 6b (right), shows that the developed adhesive coating process closes a quarter of the gap between the untreated, recycled rubber, and virgin rubber. The gap in mechanical performance as a result of the presence of once-vulcanized rubber is depicted in the area between lines demarcating maximum stress and strain at break for uncoated GRP negative control and virgin rubber positive controls. The progression scale was defined by setting the stress at break for the uncoated GRP and no-particle (base) control to 0% (σ_0) and 100% (σ_{100}), respectively. The progress percentage is thus defined as $P = (\sigma - \sigma_0)/(\sigma_{100} - \sigma_0)$, where σ is the stress at break for each coated sample. The progress percentage for the coated samples ranges from 14 to 25%, demonstrating the widespread utility of the coating process. For 16 samples, the stress-at-break improvements were achieved with no significant loss in elongation at break, suggesting that formulation and process optimizations can enable improvements in both properties, which are typically mutually exclusive.[69]

The simplifications made to the coating and reblending process in the trial level do not negatively affect performance vs the base-case parameters in GRP-containing samples (see Supporting Information XVI for p-values). The coated sample with all five trial-level parameters had a higher progress percentage ($P = 22\%$) than that with all five base-case parameters ($P = 19\%$), though these differences are not statistically significant (Supporting Information XVI). Interestingly, the trial-level conditions result in a much lower toughness, stress at break ($P = 58\%$), and elongation at break ($p < 0.01$) than the base case in the no-particle controls (Figure 6a). These results suggest that when the rubber is mixed without GRPs, the longer mixing duration in the trial level does not fully compensate in terms of mixing quality for the lower mixing speed vs the base-case conditions. Once GRPs are introduced, however, the lower mixing speed used in the trial level may preserve more of the SCA coating on the particle surface, helping to offset performance losses resulting from imperfect mixing. These findings are quite promising, as the trial-level process uses less cement, does not require precuring, and employs a single mixing speed at each step.

The Yates statistical algorithm was then applied to the full data set, confirming that the trial-level parameters are unlikely to be detrimental to performance once particles are introduced into the reblending scheme. The algorithm was used to estimate the impact of each factor or combinations therein in the 2^5 factorial design.[70] All effects were smaller than the average standard error of each metric (stress and elongation at break, toughness), giving t-values less than unity that were not statistically significant (Supporting Information XVI). Though the Yates statistical algorithm did not identify any influential factors on material performance, it does reinforce findings from the laminate studies, which suggested that bond strength was insensitive to formulation parameters over a wide range of cement concentrations and solids' areal densities. The relative insensitivity of the performance gains to the SCA formulation and processing parameters indicates that the greatly simplified, more cost-effective trial-level procedure can be implemented without sacrificing performance. As such, the laminate and particle studies in aggregate give strong evidence that the performance improvements gained with the SCA are robust to parameter variability, making this technology more easily scalable and commercially viable.

A few other authors have performed similar controlled studies of GRP reblending using different methods. Mangili et al.[71] compared three devulcanization methods (use of supercritical CO_2, ultrasonic treatment, and biological desulfurization) of GRP, reblended in raw natural rubber at a loading of 10 phr. The best sample had a tensile strength value of 80% of that of all NR controls, compared to the best sample of the current study at 52% of the base trial controls. The better performance of their samples is to be expected

https://doi.org/10.1021/acsapm.0c01343
ACS Appl. Polym. Mater. 2021, 3, 4849−4860

given the lower loading in GRP. Hassan et al.[51] studied the effect of γ irradiation on GRP reblended with acrylonitrile-butadiene rubber. They explored GRP loadings from 0 to 80 wt % with different irradiation levels. When looking at tensile strength, their best-performing sample is the 80 wt % GRP blend with the highest radiation dose, it retains close to 90% of the all acrylonitrile-butadiene rubber control. On the other hand, elongation at break is reduced to less than 20% of the control value. Even with this great tensile strength retention, the absolute values do not exceed 3 MPa. Furthermore, neither of the studies attempted to reblend the GRP in the same rubber composition. As the early failure of the rubber blends studied in the current paper is due to the sharp difference of mechanical properties between the overly cross-linked GRP and ideal cross-linked surrounding matrix, a GRP composite with a different polymer matrix could, in part, compensate for the difference in mechanical properties.

4. CONCLUSIONS

The mechanical strength and performance of rubber compounds containing recycled rubber particles are significantly improved by treating the particle surface with newly developed single-component adhesives (SCAs). Flat rubber laminates treated with a two-component adhesive (TCA) demonstrated that bonding between vulcanized and unvulcanized rubber surfaces can be significantly improved through adhesive application. An SCA was then developed from blends of cushion gum and cement to enable simplified adhesive processing that would be compatible with particle coating. Substantial improvements in interfacial bonding between vulcanized and virgin rubbers were confirmed by both TCA and SCA applications. Several SCA formulations achieved 75% of the bond strength of fresh rubber compound, confirming the utility of the SCA.

When the SCA was applied to the surface of rubber particles prior to reblending with the virgin compound, statistically significant improvements in stress at break and toughness were gained for several recycled GRP formulations, with minimal or no detrimental impact on extensibility. In the best treatments, these two metrics improve almost 50% vs the untreated controls, and roughly one-quarter of the performance gap between untreated recycled rubber and particle-free virgin compound is closed. The performance gains are substantial despite the high particle loading (15 fractions) than the untreated GRP with equivalent performance. Both the flat laminate and particle studies demonstrate that the performance gains are robust to variations in formulation and processing conditions over wide parameter ranges. Thus, by minimizing the number of adhesive components and the number and complexity of processing steps, a simple and cost-effective method of rubber recycling has been developed, which is compatible with and incorporable into the existing rubber recycling infrastructure.

■ ASSOCIATED CONTENT

Supporting Information

The Supporting Information is available free of charge at https://pubs.acs.org/doi/10.1021/acsapm.0c01343.

Peel adhesion test data, tensile test raw data, sample torque curves during particle coating and reblending, laminate surfaces after mechanical testing, and TGA degradation profiles (PDF)

■ AUTHOR INFORMATION

Corresponding Author

Bradley D. Olsen − *Department of Chemical Engineering, Massachusetts Institute of Technology, Cambridge, Massachusetts 02139, United States;* orcid.org/0000-0002-7272-7140; Email: bdolsen@mit.edu

Authors

Michelle A. Calabrese − *Department of Chemical Engineering, Massachusetts Institute of Technology, Cambridge, Massachusetts 02139, United States;* Present Address: Department of Chemical Engineering and Materials Science, University of Minnesota, Minneapolis, Minnesota 55455, United States; orcid.org/0000-0003-4577-6999

Wui Yarn Chan − *Department of Chemical Engineering, Massachusetts Institute of Technology, Cambridge, Massachusetts 02139, United States;* Present Address: Department of Chemistry, University of Minnesota, Minneapolis, Minnesota 55455, United States.

Sarah H. M. Av-Ron − *Department of Chemical Engineering, Massachusetts Institute of Technology, Cambridge, Massachusetts 02139, United States*

Complete contact information is available at: https://pubs.acs.org/10.1021/acsapm.0c01343

Author Contributions

The manuscript was written through contributions of all authors. All authors have given approval to the final version of the manuscript.

Funding

This research was funded by NSF SBIR Grant 1820122 and the MIT Tata Center for Technology and Design.*

Notes

The authors declare no competing financial interest.

■ ACKNOWLEDGMENTS

The authors thank the MIT Tata Center for Technology and Design. The authors thank Georg Bohm for supplying rubber materials, including GRP, laminate strips, and MB for reblending experiments.

■ ABBREVIATIONS

AS, average strength; CG, cushion gum; GPC, gel phase chromatography; GRP, ground rubber particle; MP, maximum peak; AP, average peak; SCA, single-component adhesive; TCA, two-component adhesive

■ REFERENCES

(1) Smith, M. N. The number of cars will double worldwide by 2040. https://www.businessinsider.com/global-transport-use-will-double-by-2040-as-china-and-india-gdp-balloon?r=UK&IR=T, 2016.

(2) Tomassini, B. R. A Tire Story. https://blog.epa.gov/2009/03/26/a-tire-story/, 2009.

(3) Sunthonpagasit, N.; Duffey, M. R. Scrap tires to crumb rubber: feasibility analysis for processing facilities. *Resour., Conserv. Recycl.* **2004**, *40*, 281−299.

(4) Weissman, S. L.; Sackman, J. L.; Gillen, D.; Monismith, C. *Extending the Lifespan of Tires: Final Report*, 2003.

(5) Rubber Manufacturing Association. *9th Biennial Report on Scrap Tire Markets in the US*; 2009.

(6) US Tire Manufacturing Association. Ground rubber markets 2017, 2017. http://www.ustires.org/system/files/USTMA_summ_2017_072018.pdf.
(7) Luo, T.; Isayev, A. I. Rubber/Plastic Blends Based on Devulcanized Ground Tire Rubber. *J. Elastomers Plast.* **1998**, *30*, 133−160.
(8) Dick, J. S. Rubber Technology and Testing for Achieving Product Performance. *India Rubber Expo course material*, 2017.
(9) Tripathy, A. R.; Morin, J. E.; Williams, D. E.; Eyles, S. J.; Farris, R. J. A novel approach to improving the mechanical properties in recycled vulcanized natural rubber and its mechanism. *Macromolecules* **2002**, *35*, 4616−4627.
(10) Bilgili, E.; Dybek, A.; Arastoopour, H.; Bernstein, B. A New Recycling Technology: Compression Molding of Pulverized Rubber Waste in the Absence of Virgin Rubber. *J. Elastomers Plast.* **2003**, *35*, 235−256.
(11) Kim, J. K. Utilization of Recycled Crumb Rubber as a Compounding Tool. *Int. Polym. Process.* **1998**, *13*, 358−364.
(12) Formela, K.; Wąsowicz, D.; Formela, M.; Hejna, A.; Haponiuk, J. Curing characteristics, mechanical and thermal properties of reclaimed ground tire rubber cured with various vulcanizing systems. *Iran. Polym. J.* **2015**, *24*, 289−297.
(13) Adhikari, B.; De, D.; Maiti, S. Reclamation and recycling of waste rubber. *Prog. Polym. Sci.* **2000**, *25*, 909−948.
(14) Kim, S. W.; Park, H. Y.; Seo, K. H. Effects of cure systems of ground rubber and rubber matrix on their adhesion and crosslink structures. *Rubber Chem. Technol.* **2006**, *79*, 806−819.
(15) Myhre, M.; Saiwari, S.; Dierkes, W.; Noordermeer, J. Rubber Recycling: Chemistry, processing, and applications. *Rubber Chem. Technol.* **2012**, *85*, 408−449.
(16) Amari, T.; Themelis, N. J.; Wernick, I. K. Resource recovery from used rubber tires. *Resources Policy* **1999**, *25*, 179−188.
(17) Goldshtein, V.; Kopylov, M. Method and Composition for Devulcanization of Waste Rubber. U.S. Patent US6,541,526B12003.
(18) Burford, R. P.; Pittolo, M. The mechanical properties of rubber compounds containing soft fillers - Part 1 Tensileproperties and fracture morphology. *J. Mater. Sci.* **1984**, *19*, 3059−3067.
(19) De, D.; Maiti, S.; Adhikari, B. Reclaiming of rubber by a renewable resource material (RRM). III. Evaluation of properties of NR reclaim. *J. Appl. Polym. Sci.* **2000**, *75*, 1493−1502.
(20) Kojima, M.; Tosaka, M.; Ikeda, Y.; Kohjiya, S. Devulcanization of carbon black filled natural rubber using supercritical carbon dioxide. *J. Appl. Polym. Sci.* **2005**, *95*, 137−143.
(21) Tao, G.; He, Q.; Xia, Y.; Jia, G.; Yang, H.; Ma, W. The effect of devulcanization level on mechanical properties of reclaimed rubber by thermal-mechanical shearing devulcanization. *J. Appl. Polym. Sci.* **2013**, *129*, 2598−2605.
(22) Kim, J. K.; Park, J. W. The Biological and Chemical Desulfurization of Crumb Rubber for the Rubber Compounding. *Appl. Polym. Sci.* **1999**, *72*, 1543−1549.
(23) Sato, S.; et al. Microbial scission of sulfide linkages in vulcanized natural rubber by a white rot basidiomycete, Ceriporiopsis subvermispora. *Biomacromolecules* **2004**, *5*, 511−515.
(24) Zanchet, A.; et al. Characterization of Microwave-Devulcanized Composites of Ground SBR Scraps. *J. Elastomers Plast.* **2009**, *41*, 497−507.
(25) Garcia, P. S.; de Sousa, F. D. B.; de Lima, J. A.; Cruz, S. A.; Scuracchio, C. H. Devulcanization of ground tire rubber: Physical and chemical changes after different microwave exposure times. *eXPRESS Polym. Lett.* **2015**, *9*, 1015−1026.
(26) Isayev, A. I.; Yushanov, S. P.; Kim, S.-H.; Levin, V. Y. Ultrasonic devulcanization of waste rubbers: Experimentation andmodeling. *Rheol. Acta* **1996**, *35*, 616−630.
(27) Diao, B.; Isayev, A. I.; Levin, V. Y. Basic study of continuous ultrasonic devulcanization of unfilled silicone rubber. *Rubber Chem. Technol.* **1999**, *72*, 152−164.
(28) Yushanov, S. P.; Isayev, A. I.; Kim, S. H. Ultrasonic devulcanization of SBR rubber: Experimentation and modeling based on cavitation and percolation theories. *Rubber Chem. Technol.* **1998**, *71*, 168−190.
(29) Rader, C. P.; Baldwin, S. D.; Cornell, D. D.; Sadler, G. D.; Stockel, R. F. In *Plastic, Rubber and Paper Recycling*, ACS Symposium Series, American Chemical Society,: Washington DC, 1995.
(30) Jana, G. K.; Das, C. K. Devulcanization of Natural Rubber Vulcanizates by Mechanochemical Process. *Polym.-Plast. Technol. Eng.* **2005**, *44*, 1399−1412.
(31) Vega, B.; Montero, L.; Lincoln, S.; Agulló, N.; Borrós, S. Control of vulcanizing/devulcanizing behavior of diphenyl disulfide with microwaves as the heating source. *J. Appl. Polym. Sci.* **2008**, *108*, 1969−1975.
(32) Thaicharoen, P.; Thamyongkit, P.; Poompradub, S. Thiosalicylic acid as a devulcanizing agent for mechano-chemical devulcanization. *Korean J. Chem. Eng.* **2010**, *27*, 1177−1183.
(33) Jana, G. K.; Mahaling, R. N.; Das, C. K. A novel devulcanization technology for vulcanized natural rubber. *J. Appl. Polym. Sci.* **2006**, *99*, 2831−2840.
(34) Walvekar, R.; Zulkefly, M. A.; Ramarad, S.; Siddiqui, K. Devulcanization of waste tire rubber using Amine Based Solvents and Ultrasonic Energy. *MATEC Web Conf.* **2018**, *152*, No. 01007.
(35) Dijkhuis, K. A. J. Recycling of Vulcanized EPDM-Rubber: Mechanistic Studies into the Development of a Continuous Process Using Amines as Devulcanization Aids Ph.D. Thesis, University of Twente, 2008.
(36) Kormer, V. A.; Sekhar, B. C. *Forbedringer i og relaterende til regenerering af naturlige og syntetiske gummier*, 1994.
(37) Zhang, X.; Lu, C.; Liang, M. Properties of natural rubber vulcanizates containing mechanochemically devulcanized ground tire rubber. *J. Polym. Res.* **2009**, *16*, 411−419.
(38) Warner, W. C. Methods of Devulcanization. *Rubber Chem. Technol.* **1994**, *67*, 559−566.
(39) Kojima, M.; Ogawa, K.; Mizoshima, H.; Tosaka, M.; Kohjiya, S.; Ikeda, Y. Devulcanization of Sulfur-Cured Isoprene Rubber in Supercritical Carbon Dioxide. *Rubber Chem. Technol.* **2003**, *76*, 957−968.
(40) Zhang, Q.; Tzoganakis, C. In *Devulcanization of Recycled Tire Rubber Using Supercritical Carbon Dioxide*, Global Plastics Environmental Conference, 2004.
(41) Bhayani, P. Site visit to Kiran Rubber Industries: Maharashtra, India.
(42) Ghavipanjeh, F.; Ziaei Rad, Z.; Pazouki, M. Devulcanization of Ground Tires by Different Strains of Bacteria: Optimization of Culture Condition by Taguchi Method. *J. Polym. Environ.* **2018**, *26*, 3168−3175.
(43) Chritiansson, M.; Stenberg, B.; Wallenberg, L. R.; Holst, O. Reduction of surface sulphur upon microbial devulcanization of rubber materials. *Biotechnol. Lett.* **1998**, *20*, 637−642.
(44) Ramarad, S.; Khalid, M.; Ratnam, C. T.; Chuah, A. L.; Rashmi, W. Waste tire rubber in polymer blends: A review on the evolution, properties and future. *Prog. Mater. Sci.* **2015**, *72*, 100−140.
(45) Fazli, A.; Rodrigue, D. Waste rubber recycling: A review on the evolution and properties of thermoplastic elastomers. *Materials* **2020**, *13*, No. 782.
(46) Ning, N.; Li, S.; Wu, H.; Tian, H.; Yao, P.; Hu, G.-H.; Tian, M.; Zhang, L. Preparation, microstructure, and microstructure-properties relationship of thermoplastic vulcanizates (TPVs): A review. *Prog. Polym. Sci.* **2018**, *79*, 61−97.
(47) Kim, J. I.; Ryu, S. H.; Chang, Y. W. Mechanical and dynamic mechanical properties of waste rubber powder/HDPE composite. *J. Appl. Polym. Sci.* **2000**, *77*, 2595−2602.
(48) Lee, S. H.; Zhang, Z. X.; Xu, D.; Chung, D.; Oh, G. J.; Kim, J. K. Dynamic Reaction Involving Surface Modified Waste Ground Rubber Tire Powder/Polypropylene. *Polym. Eng. Sci.* **2009**, *49*, 168−176.
(49) Rezaei Abadchi, M.; Arani, A. J.; Nazockdast, H. Partial Replacement of NR by GTR in Thermoplastic Elastomer Based on LLDPE/NR Through Using Reactive Blending: Its Effects on

https://doi.org/10.1021/acsapm.0c01343
ACS Appl. Polym. Mater. 2021, 3, 4849−4860

Morphology, Rheological, and Mechanical Properties. *J. Appl. Polym. Sci.* **2010**, *115*, 2416−2422.
(50) Colom, X.; Cañavate, J.; Carrillo, F.; Suñol, J. J. Effect of the Particle Size and Acid Pretreatments on Compatibility and Properties of Recycled HDPE Plastic Bottles Filled with Ground Tyre Powder. *J. Appl. Polym. Sci.* **2009**, *112*, 1882−1890.
(51) Hassan, M. M.; Aly, R. O.; El-Ghandour, A. H.; Abdelnaby, H. A. Effect of gamma irradiation on some properties of reclaimed rubber/nitrile-butadiene rubber blend and its swelling in motor and brake oils. *J. Elastomers Plast.* **2013**, *45*, 77−94.
(52) Tantayanon, S.; Juikham, S. Enhanced toughening of poly(propylene) with reclaimed-tire rubber. *J. Appl. Polym. Sci.* **2004**, *91*, 510−515.
(53) Lu, X.; Wang, W.; Yu, L. Waste ground rubber tire powder/thermoplastic vulcanizate blends: Preparation, characterization, and compatibility. *J. Appl. Polym. Sci.* **2014**, *131*, 1−9.
(54) Rocha, M. C. G.; Leyva, M. E.; De Oliveira, M. G. Thermoplastic elastomers blends based on linear low density polyethylene, ethylene-1-octene copolymers and ground rubber tire. *Polímeros* **2014**, *24*, 23−29.
(55) Li, Y.; Zhang, Y.; Zhang, Y. Morphology and mechanical properties of HDPE/SRP/elastomer composites: Effect of elastomer polarity. *Polym. Test.* **2004**, *23*, 83−90.
(56) Li, Y.; Zhang, Y.; Zhang, Y. X. Structure and mechanical properties of SRP/HDPE/POE (EPR or EPDM) composites. *Polym. Test.* **2003**, *22*, 859−865.
(57) Lima, P.; Oliveira, J.; Costa, V. Partial replacement of EPDM by GTR in thermoplastic elastomers based on PP/EPDM: Effects on morphology and mechanical properties. *J. Appl. Polym. Sci.* **2014**, *131*, 1−10.
(58) Cañavate, J.; Casas, P.; Colom, X.; Nogués, F. Formulations for thermoplastic vulcanizates based on high density polyethylene, ethylene-propylene-diene monomer, and ground tyre rubber. *J. Compos. Mater.* **2011**, *45*, 1189−1200.
(59) Pittolo, M.; Burford, R. P. Recycled Rubber Crumb As A Toughener Of Polystyrene. *Rubber Chem. Technol.* **1985**, *58*, 97−106.
(60) Kim, J. K.; Burford, R. P. Study on powder utilization of waste tires as a filler in rubber compounding. *Rubber Chem. Techno.l* **1998**, *71*, 1028−1041.
(61) Adam, G.; Sebenik, A.; Osredkar, U.; Ranogajec, F.; Veksli, Z. Possibility of using grafted waste rubber. *Rubber Chem. Technol.* **1991**, *64*, 133−138.
(62) Carver, R. J. Method and Bonding Agent for Retreading Pneumatic Tire Casings. U.S. Patent US3136673A1964.
(63) Ferrer, G. Economics of tire remanufacturing. *Resour. Conserv. Recycl.* **1997**, *19*, 221−255.
(64) Mathew, G.; Singh, R. P.; Nair, N. R.; Thomas, S. Recycling of natural rubber latex waste and its interaction in epoxidised natural rubber. *Polym. Degrad. Stab.* **2001**, *42*, 2137−2165.
(65) Sener, J.-Y.; Delannay, F. On the transition between adhesive and cohesive modes of debonding during peeling of thin plates bonded with an epoxide adhesive. *Int. J. Adhes. Adhes.* **2001**, *21*, 339−348.
(66) Gent, A. N.; Petrich, R. P. Adhesion of Viscoelastic Materials To Rigid Substrates. *Proc. R. Soc. London, Ser. A* **1969**, *310*, 433−448.
(67) Aubrey, D. W.; Welding, G. N.; Wong, T. Failure mechanisms in peeling of pressure-sensitive adhesive tape. *J. Appl. Polym. Sci.* **1969**, *13*, 2193−2207.
(68) Erman, B.; Mark, J. E.; Roland, C. M. *The Science and Technology of Rubber*, 4th ed.; Elsevier: Isayev, A. I., 2013; Chapter 15, pp 697−764.
(69) Ritchie, R. O. The conflicts between strength and toughness. *Nat. Mater.* **2011**, *10*, 817−822.
(70) Box, G. E. P.; Hunter, W. G.; Hunter, J. S. *Statistics For Experimenters: An Introduction to Design, Data Analysis, and Model Building*; John Wiley and Sons, 1978.
(71) Mangili, I.; et al. Mechanical and rheological properties of natural rubber compounds containing devulcanized ground tire rubber from several methods. *Polym. Degrad. Stab.* **2015**, *121*, 369−377.

https://doi.org/10.1021/acsapm.0c01343
ACS Appl. Polym. Mater. 2021, 3, 4849−4860